Journal of Nuclear Medicine, published on June 9, 2022 as doi:10.2967/jnumed.121.263773

Original article

Intraoperative molecular fluorescence imaging of pancreatic cancer by targeting vascular endothelial growth factor: A multicenter feasibility dose-escalation study

Babs G. Sibinga Mulder, MD, PhD[1]*, Marjory Koller, MD, PhD[2*], Evelien W. Duiker, MD, PhD[3], Arantza Farina Sarasqueta, MD, PhD[4], J. Burggraaf, MD, PhD[5], Vincent E. de Meijer, MD, PhD[2], Alexander L. Vahrmeijer, MD, PhD[1], Frederik J.H. Hoogwater, MD, PhD[2], Bert A. Bonsing, MD, PhD[1], Gooitzen M. van Dam, MD, PhD[2,6], J. Sven D. Mieog, MD, PhD[1], Bobby K. Pranger, MD[2]

[1] *Department of Surgery, Leiden University Medical Center, Leiden, the Netherlands.*

[2] *Department of Surgery, University of Groningen and University Medical Center Groningen, Groningen, the Netherlands.*

[3] *Department of Pathology and Medical Biology, University Medical Center Groningen, Groningen, the Netherlands.*

[4] *Department of Pathology, Leiden University Medical Center, Leiden, the Netherlands.*

[5] *Center for Human Drug Research, Leiden, the Netherlands*

[6] *AxelaRx / TRACER Europe BV, Groningen, The Netherlands*

**Shared authorship*

Corresponding Author:

Bobby K. Pranger, MD, University Medical Center Groningen, Hanzeplein 1 – Ba33, 9700 RB, Groningen, The Netherlands. Email: b.k.pranger@umcg.nl. phone: +31 (0)50-36 14204

First authors: Babs G. Sibinga Mulder, MD, PhD and M. Koller, MD, PhD, Leiden University Medical Center and University Medical Center Groningen, PO box 9600, 2300 RC Leiden, the Netherlands and Hanzeplein 1 – Ba33, 9700 RB Groningen, the Netherlands. E-mail: b.g.sibinga_mulder@lumc.nl and m.koller@umcg.nl

Disclosure: The research leading to the results was supported by an unrestricted research grant from SurgVision BV. The authors M.K. and G.M.V.D. report receiving grants from the FP-7 Framework Programme Betacure grant no. 602812, during the study. This work was supported by the Bas Mulder Award (grant UL2015-7665) from the Dutch Cancer Society. No other potential conflicts of interest relevant to this article exist.

Running title: Fluorescence imaging of the pancreas

Word count abstract: 250

Word count main text: 3250

ABSTRACT

Rationale

Tumor visualization with near-infrared fluorescence (NIRF) imaging could aid exploration and resection of pancreatic cancer by visualizing the tumor in real time. Conjugation of the near-infrared fluorophore IRDye800CW to the monoclonal antibody bevacizumab enables targeting of vascular endothelial growth factor-A (VEGF-A). The aim of this study was to determine if intraoperative tumor-specific imaging of pancreatic cancer with the fluorescent tracer bevacizumab-800CW is feasible and safe.

Materials and Methods

In this multicenter, dose escalation phase I trial patients with suspicion of pancreatic ductal adenocarcinoma (PDAC) were administered bevacizumab-800CW (4.5mg, 10mg or 25mg) three days before surgery. Safety monitoring encompassed allergic or anaphylactic reactions and serious adverse events attributed to bevacizumab-800CW. Intraoperative NIRF imaging was performed immediately after laparotomy, just before and after resection of the specimen. Postoperatively, fluorescence signals on the axial slices and formalin-fixed paraffin-embedded tissue blocks from the resected specimens were correlated to histology. Subsequently, tumor-to-background ratios (TBR) were calculated.

Results

Ten patients with clinically suspected PDAC were enrolled in the study. Four of the resected specimens were confirmed PDACs; other malignancies were distal cholangiocarcinoma, ampullary carcinoma and neuroendocrine tumors. No serious adverse events were related to bevacizumab-800CW. *In vivo* tumor visualization with NIRF imaging differed per tumor type and was non-conclusive. *Ex vivo* TBRs were 1.3, 1.5 and 2.5 for 4.5mg, 10mg and 25mg groups, respectively.

Conclusion

NIRF guided surgery in patients with suspect PDAC using bevacizumab-IRDye800CW is feasible and safe. However, suboptimal TBRs were obtained because no clear distinction between pancreatic cancer from normal or inflamed pancreatic tissue was achieved. Therefore, a more tumor-specific tracer other than bevacizumab-IRDye800CW for PDAC is preferred.

Key words: near-infrared fluorescence imaging, molecular fluorescence imaging, pancreatic cancer.

INTRODUCTION

Currently, the only curative treatment of pancreatic cancer is radical surgery (R0 resection). However, a radical resection is achieved in a minority of the patients. Surgery with curative intent may be aborted during the procedure when exploratory laparotomy reveals locally advanced disease (e.g., arterial encasement) or distant metastases (*1*,*2*). Due to the quick spread of pancreatic cancer cells via perineural and perivascular pathways, occult metastases and tumor growth in resection margins can easily be missed (*3*). Besides intraoperative frozen section analysis and ultrasonography, surgeons typically rely on visual inspection and palpation alone to distinguish between tumorous and benign tissue and to detect remaining small tumor deposits or locoregional metastases. Because of these limitations, positive resection margin rates are reported as high as 50%-75% (*4*).

Improved visualization of resection margins and detection of small tumor deposits is highly desirable in pancreatic cancer surgery in order to prevent under- or overtreatment. A relatively new technique that can fulfill this unmet need is intraoperative near-infrared fluorescence (NIRF) imaging (*5*). The main advantages of NIRF imaging are the real-time and ideally tumor-specific visual feedback to the surgeon, thereby enabling differentiation between benign and malignant tissue during surgery and enhancing visualization of small tumor deposits (*6*). A tumor-specific fluorescent tracer will accumulate in or bind to the tumor after intravenous administration. Subsequently, fluorescence signals can be detected using dedicated imaging systems. Recent studies showed promising results using tumor-specific NIRF imaging for the visualization of several cancer types (*7–10*). However, successful and tumor-specific visualization of pancreatic cancer using NIRF imaging remains challenging due to several factors such as the presence of the often present desmoplastic stroma reaction or peri-inflammatory tissue reaction.

Vascular Endothelial Growth Factor (VEGF) is involved in tumor-induced angiogenesis and lymph angiogenesis in most solid tumors (*11*). Several studies report an overexpression of VEGF in pancreatic cancer tissue compared to normal pancreatic tissue (*12*,*13*). Bevacizumab is an antibody directed towards VEGF-A overexpressing tumors and by coupling the antibody to the organic fluorophore IRDye800CW a tumor-specific NIRF tracer (bevacizumab-800CW) was developed. Bevacizumab-800CW has already shown to be a valid and safe tracer for molecular imaging in several solid cancer types (*8*,*9*,*14*,*15*).

The aim of this study was to determine whether intraoperative tumor-specific imaging of pancreatic cancer is feasible and safe using the fluorescent tracer bevacizumab-800CW.

MATERIALS AND METHODS

Patient Population

This study was approved by the certified medical ethics review board of the University Medical Center Groningen and Leiden University Medical Center (clinicaltrials.gov ID: NCT02743975). The study was performed in accordance to the ethical principles of Helsinki (adapted version Fortaleza, Brazil, 2013) and the laws and regulations of the Netherlands. All patients provided written informed consent before participation in the study. A safety monitoring board was appointed before start of the clinical trial. All serious adverse events occurring during or after surgery were reported immediately to the investigational review board of the University Medical Center Groningen, the data safety monitoring board, and the Dutch Central Committee on Research Involving Human Subjects.

Patients aged older than 18 years with a clinical suspicion of pancreatic ductal adenocarcinoma (PDAC), who were scheduled to undergo surgical intervention with curative intent were included for this single arm, open-label, multi-center study. All patients had a World Health Organisation performance score of 0-2. Patients who underwent neoadjuvant treatment or had a concurrent invasive malignancy were excluded. Other exclusion criteria were: medical or psychiatric conditions compromising the patient's ability to give informed consent, pregnant or lactating women, a history of infusion reactions to bevacizumab, inadequately controlled hypertension or a history of myocardial infarction, transient ischemic attack, cerebrovascular accidents, pulmonary embolism, uncontrolled chronic hepatic failure or unstable angina pectoris six months prior to inclusion.

Study Design

The primary objective of this study was to identify the optimal dose for the visualization of tumor tissue. The secondary objective was to determine whether bevacizumab-800CW could be used safely to identify pancreatic ductal adenocarcinoma with NIRF imaging

Therefore, a 4 x 3 dose-finding study design was used, consisting of two parts. Part I consisted of four intravenously administered ascending doses of 4.5mg, 10mg, 25mg, and 50mg bevacizumab-800CW three days prior to the planned surgery to three patients each. In part II, the defined optimal dose group would be supplemented to ten patients in order to obtain a sufficient number of data points. The most optimal dose group would be chosen on the basis of *ex-vivo* tumor-to-background ratio (TBR). Interim analyses were performed after completion of each cohort for the evaluation of intraoperative fluorescence signals, analyses of the *ex vivo* tumor-to-background ratios and safety outcomes.

Bevacizumab-IRDye800CW

Bevacizumab-IRDye800CW was produced in the Good Manufacturing Practice certified facility of the University Medical Center Groningen Hospital Pharmacy by conjugating bevacizumab (Roche AG, Basel, Switzerland) and IRDye-800CW-NHS (LI-COR Biosciences Inc, Lincoln, NE, USA) under regulated conditions (*16*). IRDye800CW has excitation/emission maxima at 774 nm/789 nm.

Imaging Systems

Intraoperative imaging was done with a fluorescence camera system dedicated to detect IRDye-800CW-NHS (SurgVision BV, Groningen, the Netherlands). The system was configured with two light emitting diode lights for 800 nm illumination and one light emitting diode light for white light

illumination. Real-time color and NIRF images were simultaneously collected. The imaging device was approved for intraoperative application in humans by the technical departments of the University Medical Center Groningen and Leiden University Medical Center. *Ex vivo* imaging was performed using the Blackbox (SurgVision BV, Groningen, the Netherlands) or the Pearl imager (LI-COR Biosciences Inc., Lincoln, NE, USA). For detection of fluorescence in Formalin-Fixed Paraffin-Embedded (FFPE) blocks the Odyssey® CLX fluorescence flatbed scanning system (LI-COR Biosciences Inc., Lincoln, NE, USA) was used.

Procedures

Figure 1 provides an overview of the workflow of NIRF imaging during all study steps as based on a proposed standardization protocol (*9*). Prior to surgery, all patients underwent staging laparoscopy to exclude locally advanced or metastatic disease stage. Patients received bevacizumab-800CW three days before surgery as an intravenous bolus injection. Tolerability assessments (electrocardiogram, blood pressure, pulse, peripheral oxygen saturation, respiratory rate and temperature), were performed just before tracer injection, shortly after tracer injection and one hour after tracer injection.

Surgery was performed according to standard practice. Surgeons were not allowed to excise additional tissue based exclusively on fluorescence signals detected intraoperatively. NIRF imaging was performed at three predefined time points: (1) after laparotomy during which all surrounding organs were imaged and fluorescence intensity was determined, and in case nonspecific background fluorescence signals were present these were noted, (2) after full preparation of the specimen just before resection, the fluorescence intensity of the expected tumor and the normal pancreatic tissue was noted, and (3) after resection of the specimen, during which the remaining tissue was imaged. If additional lesions were detected with the near infrared camera

system that were not part of intended resection, the surgeon was allowed to perform a biopsy for postoperative pathological analysis.

After resection, the gross specimen was imaged. After formalin fixation the specimen was sliced in 0,3 – 0,5 cm thick slices according to the preferred protocol (*4*,*17*). All slices were macroscopically examined and imaged. Those slices considered relevant for the pathologist were processed for histological assessment. The selection of tissue for embedding in formalin-fixed paraffin-embedded (FFPE) blocks was not altered by fluorescence signal. However, after the pathologist completed the selection of slices for diagnostic purposes, an additional slice with high fluorescence signal that was not initially selected by the pathologist as relevant, could be embedded apart from standard-of-care. We did VEGF staining on 4 μm tissue slides of FFPE tissue blocks containing both tumor and background tissue in all patients (see Supplemental information). After microscopic evaluation and the final pathology report, the FFPE blocks were imaged and the TBRs were determined on the fluorescence images of the FFPE blocks after correlation of regions of interest on the corresponding histological slice. Additional information about the tracer, imaging procedures and pathological processing is provided in the Supplementary Information.

Fluorescence Quantification

Ex vivo TBRs were calculated on fresh serially sliced tissues (so-called bread-loaf slices). The tumor and the surrounding non-tumor tissue were precisely delineated on standard H&E histopathologic slides by a pathologist masked to fluorescence. An overlay with fluorescent tissue slices was based on anatomic landmarks. Afterwards, the ex vivo TBR was calculated as the mean fluorescence intensity (MFI, arbitrary unit) of pancreatic cancer tissue divided by the MFI of the background. The background MFI was calculated on all nontumor tissue for every tissue slice.

Statistics

Descriptive statistics were reported as means with standard deviation, whereas median with range was used in case of a skewed distribution. Fluorescence signals in tumor and normal tissue was compared using the Mann-Whitney test. A *P*-value of <0.05 was considered statistically significant. For descriptive statistics SPSS (version 23.0) was used, graphs were designed with Graphpad Prism (version 7.0).

RESULTS

Patient and Safety Data

Between December 1, 2016, and February 26, 2018, ten patients were enrolled with suspected pancreatic ductal carcinoma. Table 1 provides an overview of patient characteristics and tumor characteristics per patient (patient 01-10). After completion of the 4.5mg, 10mg and 25 mg dose groups in part I of the study, the investigational review board mandated termination of the study, because of low TBRs. In nine patients, the tracer was administered three days before surgery. In patient 03 imaging was performed 10 days after administration of 4.5mg tracer due to a postponed exploration because of an adverse event the day before surgery. Therefore, one additional patient was included in the first dose group (4.5mg). No allergic or anaphylactic reactions related to bevacizumab-IRDye800CW were noted. Two serious adverse events were reported, both of which developed in patient 05 and were attributed to the pancreatoduodenectomy. These included a pancreatic fistula requiring percutaneous drainage and antibiotic treatment, and bleeding of the gastroduodenal artery stump 27 days after surgery requiring radiological coiling. All safety data is provided in Supplemental Table 1. Based on final histology of the resected specimens, various malignancies were found in the study: pancreatic ductal adenocarcinoma (n=4), distal cholangiocarcinoma (n=1), carcinoma of the ampullary region (n=2), well differentiated grade 3 neuro-endocrine tumor of the pancreas (n=1) and a low-grade intraductal papillary mucinous neoplasm (n=1). In patient 04 an auto-immune pancreatitis instead of malignancy was diagnosed on histology.

In and Ex Vivo Imaging per Tumor Type

PDAC. The approximate location of the expected primary tumor could be visualized with NIRF imaging *in vivo* with all tested doses of the tracer. However, the primary tumor was difficult

to distinguish from normal or fibrotic pancreatic tissue. After resection of the pancreatic head (in patient 06), the pancreatic tail remnant was clinically suspect for residual tumor and also showed high fluorescence. The suspicion of malignancy was confirmed by intraoperative ultrasound, and therefore the pancreatic tail was resected. Histological assessment showed a poorly differentiated tumor in the head, body and tail of the pancreas with the latter not diagnosed during the preoperative work-up. In the other PDAC patients, nonspecific fluorescence signals remained visible after resection of the pancreatic head. Histological assessment confirmed radical resection. The MFI increased with each dose group which resulted in TBRs of 1.4 (n=2), 1.7 (n=1) and 2.1 (n=1) per dose group, respectively (Figure 2). Figure 2 demonstrates the contrast between tumorous and other types of tissue based on the difference in fluorescence intensity. Representative fluorescence images per dose group of specimen slices and FFPE blocks of PDAC are shown in Figure 3. VEGF staining of the tissue slides showed moderate VEGF expression of normal pancreatic tissue and moderate to strong VEGF expression in tumor tissue of well or moderately differentiated cancers. In poorly differentiated tumor tissue, the VEGF expression was weak (Figure 4, 5 and 6).

Distal cholangiocarcinoma. We could not visualize fluorescence signals at the site where the tumor was expected *in vivo* (patient 01, 4.5mg). On the specimen slices and FFPE blocks, the MFI was similar between tumor and normal tissue which resulted in a TBR of 1.0 (Figure 2). VEGF staining of the tissue slides showed moderate VEGF expression of both tumor tissue and normal pancreatic tissue (Figure 4).

Carcinoma of the ampullary region. The location of the expected primary tumor could be visualized with NIRF imaging in two patients administered with either 10mg and 25mg of the tracer *in vivo*. In patient 08, tumor invasion in the superior mesenteric vein was clinically suspected, and therefore, a wedge resection of the superior mesenteric vein was performed. NIRF imaging of

the wedge was positive. Histologic assessment of the wedge confirmed ingrowth of malignant cells in the vascular wall. On the specimen slices and FFPE blocks, the MFI was similar between tumor and normal tissue which resulted in a TBR of 1.1 and 1.7 for 10mg and 25mg, respectively (Figure 2). VEGF staining of the tissue slides showed moderate VEGF expression of normal pancreatic tissue and moderate – weak VEGF expression of tumor tissue (Figure 5 and 6).

Neuro-endocrine neoplasm. The expected location of the tumor was clearly visible with NIRF imaging *in vivo* and after resection, fluorescence signals diminished strongly. On the specimen slices and FFPE blocks, the MFI was significantly different between tumor and normal tissue (27.6 vs. 7.8, p = 0.04) which resulted in a TBR of 3.6 (Figure 2). VEGF staining of the tissue slides showed weak VEGF expression of tumor tissue and moderate VEGF expression of normal pancreatic tissue (Figure 6).

Intraductal papillary mucinous neoplasm (IPMN). The location of the expected primary tumor could be visualized with NIRF imaging *in vivo* (patient 07; 10mg), although clear distinction between pancreatic and tumorous tissue could not be made. On the specimen slices and FFPE blocks, the MFI was not significantly different between IPMN and normal tissue (84.5 vs. 56.7, p = 0.40; which resulted in a TBR of 1.5 (Figure 2). VEGF staining of the tissue slides showed moderate to strong VEGF expression of both IPMN tissue and pancreatic tissue (Figure 5).

Auto-immune pancreatitis. In patient 04 the location of the expected ‘tumor’ could be visualized with fluorescence imaging (4.5mg). With *ex vivo* histology, extensive fibrotic and inflammatory tissue was seen and no normal pancreatic tissue was found. Therefore, there was no difference in fluorescence intensity in the resected specimen of the patient with auto-immune pancreatitis (MFI 50.7). VEGF staining of the tissue slides showed weak VEGF expression of the extensive fibrotic and inflammatory tissue (Figure 4).

Ex vivo TBRs of all types of tumors together, divided per dose group, are demonstrated in Figure 2. TBRs were 1.3, 1.5 and 2.5 for 4.5mg, 10mg and 25mg, respectively. Finally, we looked into additional immunohistochemical staining with hypoxia-inducible factor 1-alpha and added two representative slides to the Supplemental Information (Supplemental Figure 1). Hypoxia-inducible factor 1-alpha staining showed a similar staining pattern as VEGF-A staining, although expression of hypoxia-inducible factor 1-alpha was less strong compared to VEGF.

DISCUSSION

In this study, the feasibility and safety of visualizing pancreatic cancer tissue with bevacizumab-800CW was assessed. Intravenous administration of bevacizumab-800CW (i.e. a flat-dose of 4.5, 10 and 25mg) three days before surgery appeared safe as no changes in safety parameters including vital signs and electrocardiogram and no related adverse events occurred. Both *in vivo* and *ex vivo* NIRF imaging of pancreatic cancer tissue was feasible with bevacizumab-800CW, as fluorescence signals could be detected in tumor tissue. However, suboptimal TBRs were obtained and reliably distinguishing pancreatic cancer tissue from normal pancreatic tissue could not be achieved.

NIRF imaging with other tracers in previous clinical trials had similar results. The feasibility of SGM-101, a monoclonal antibody against carcinoembryonic antigen labelled with 700nm fluorophore, was assessed for intraoperative NIRF imaging of PDAC. SGM-101 could reach and bind carcinoembryonic antigen expressing tumor cells, but with modest *in vivo* TBRs (1.6 for primary tumors) (*18*). With cetuximab-IRDye800 it was feasible to detect pancreatic cancer tissue and tumor-bearing lymph nodes. Studies with larger patient numbers must show if this tracer indeed is suitable for *in vivo* NIRF imaging of pancreatic cancer (*19*).

Limited success rates for treating PDAC with systemically administered agents are commonly attributed to the desmoplastic stroma of PDAC, which is thought to severely reduce the delivery of these therapies by an increased intratumoral pressure gradient and the presence of fibrotic tissue. However, cetuximab, bevacizumab and the carcinoembryonic antigen-targeting antibody are full-size monoclonal antibodies and managed to penetrate through the dense desmoplastic stroma and to bind pancreatic cancer cells and endothelial cells.

The results of these NIRF imaging studies for detection of pancreatic cancer suggest that pancreatic tumor tissue might be a difficult type to detect intraoperatively using fluorescent tracers. The yield of tumor-specific imaging in the current study was lower than expected, and therefore,

the study was terminated early. The most obvious reasons for suboptimal pancreatic cancer visualization with NIRF are unfavorable intrinsic characteristics of pancreatic cancer. Due to the previously mentioned desmoplastic stroma, poor vascularization and high intratumoral pressure, the antibody-based tracers might not accumulate optimally in the tumor as compared to the surrounding tissue. This makes it difficult to distinguish normal tissue from tumor tissue. In this study, the difficulty to demonstrate tumor-specific fluorescence imaging could also be due to a suboptimal choice of the target VEGF-A, a soluble factor present for angiogenesis in the stroma of tumor tissue. An FGmRNA profiling study on a set of normal pancreatic tissue and PDAC tissue identified THY1, CTSE, GGT5 and MUC1 as potential targets for pancreatic cancer imaging (*20*). Other targets that are potentially suitable for NIRF imaging of pancreatic tumors are integrin αvβ6 and uPAR (*21*). Furthermore, future studies should focus on a tracer that can differentiate between chemotherapy-induced fibrotic tissue and vital cancer cells, because an increased number of patients will be treated with neoadjuvant therapy. Preclinical studies showed promising results for fluorescence-guided surgery in combination with neoadjuvant chemotherapy and treatment of minimal residual cancer after fluorescence-guided surgery in pancreatic cancer (*22–24*).

Moreover, the detection of metastases is important in optimal treatment strategy assessment for pancreatic cancer patients. Identification of preoperatively missed metastases via preoperative staging laparoscopy with NIRF imaging could be of great value for these patients. Resection of the primary tumor does not increase prognosis in metastasized patients and therefore only delays appropriate treatment (*25*). In this setting a tumor-specific tracer should be used that is not metabolized by the liver, because pancreatic cancer preferably metastasizes to the liver. A potential tracer could be cRGD-ZW800-1, which is renally cleared. Preclinical studies showed promising results for pancreatic cancer detection (*26*). cRGD-ZW800-1 is currently being tested in patients with colorectal tumors and if promising will be expanded to pancreatic cancer patients

(clinicaltrials.gov ID:NL6250805817). Another promising tracer is panitumumab-IRDye800CW. This tracer proved to be safe and feasible to use for fluorescence-guided surgery in patients with pancreatic cancer undergoing surgical intervention, and has the potential to improve patient selection and enhance visualization of surgical margins, metastatic lymph nodes, and distant metastasis (*27*).

A unique aspect of our study is the variety of cancer types that were included; besides pancreatic ductal adenocarcinoma, also neuroendocrine tumors, distal cholangiocarcinoma, an IPMN and ampullary tumors were visualized with bevacizumab-800CW. Tumor targeted NIRF imaging of these tumors has not yet been described. In neuroendocrine tumors we observed a 3-fold higher signal intensity from the tumor compared to the background signal. This most likely reflects the enhanced permeability and retention effect by which high–molecular weight nontargeted drugs and prodrugs accumulate in tissues that offer increased vascular permeability.

CONCLUSION

In conclusion, NIRF guided surgery in patients with suspect pancreatic cancer using bevacizumab-IRDye800CW is feasible and safe. However, suboptimal TBRs were obtained and consequently distinguishing pancreatic cancer tissue from normal pancreatic tissue remains challenging.

KEY POINTS

Question

Is near-infrared fluorescence guided surgery using the tracer bevacizumab-800CW feasible and safe in patients with suspected pancreatic ductal adenocarcinoma?

Pertinent Findings

In this clinical trial, we show that near-infrared fluorescence guided surgery in patients with suspect pancreatic ductal adenocarcinoma using bevacizumab-800CW is feasible and safe. However, suboptimal TBRs were obtained because no clear distinction between pancreatic cancer from normal or inflamed pancreatic tissue was achieved.

Implications for Patient Care

Although suboptimal TBRs were obtained in pancreatic cancer, we showed that full-size monoclonal antibodies manage to penetrate through the dense desmoplastic stroma and to bind to pancreatic cancer cells and endothelial cells.

REFERENCES

1. Campbell F, Smith RA, Whelan P, et al. Classification of R1 resections for pancreatic cancer: the prognostic relevance of tumour involvement within 1 mm of a resection margin. *Histopathology*. 2009;55:277-83.
2. Ghaneh P, Kleeff J, Halloran CM, et al. The impact of positive resection margins on survival and recurrence following resection and adjuvant chemotherapy for Pancreatic ductal adenocarcinoma. *Ann Surg*. 2019;269:520-529.
3. Zhang J-F, Hua R, Sun Y-W, et al. Influence of perineural invasion on survival and recurrence in patients with resected pancreatic cancer. *Asian Pac J Cancer Prev*. 2013;14:5133-9.
4. Verbeke CS, Gladhaug IP. Resection margin involvement and tumour origin in pancreatic head cancer. *Br J Surg*. 2012;99:1036-1049.
5. Vahrmeijer AL, Hutteman M, van der Vorst JR, van de Velde CJH, Frangioni J V. Image-guided cancer surgery using near-infrared fluorescence. *Nat Rev Clin Oncol*. 2013;10:507-18.
6. Tipirneni KE, Warram JM, Moore LS, et al. Oncologic procedures amenable to fluorescence-guided surgery. *Ann Surg*. 2017;266:36-47.
7. Rosenthal EL, Warram JM, de Boer E, et al. Safety and tumor specificity of cetuximab-IRDye800 for surgical navigation in head and neck cancer. *Clin Cancer Res*. 2015;21:3658-66.
8. Harlaar NJ, Koller M, de Jongh SJ, et al. Molecular fluorescence-guided surgery of peritoneal carcinomatosis of colorectal origin: a single-centre feasibility study. *Lancet*

Gastroenterol Hepatol. 2016;1:283-290.

9. Koller M, Qiu S-Q, Linssen MD, et al. Implementation and benchmarking of a novel analytical framework to clinically evaluate tumor-specific fluorescent tracers. *Nat Commun*. 2018;9:3739.

10. van Dam GM, Themelis G, Crane LMA, et al. Intraoperative tumor-specific fluorescence imaging in ovarian cancer by folate receptor-α targeting: first in-human results. *Nat Med*. 2011;17:1315-9.

11. Ellis LM, Hicklin DJ. VEGF-targeted therapy: mechanisms of anti-tumour activity. *Nat Rev Cancer*. 2008;8:579-91.

12. Tang R-F, Wang S-X, Peng L, et al. Expression of vascular endothelial growth factors A and C in human pancreatic cancer. *World J Gastroenterol*. 2006;12:280-6.

13. Nagakawa Y, Aoki T, Kasuya K, Tsuchida A, Koyanagi Y. Histologic features of venous invasion, expression of vascular endothelial growth factor and matrix metalloproteinase-2 and matrix metalloproteinase-9, and the relation with liver metastasis in pancreatic cancer. *Pancreas*. 2002;24:169-78.

14. Lamberts LE, Koch M, de Jong JS, et al. Tumor-specific uptake of fluorescent bevacizumab-IRDye800CW microdosing in patients with primary breast cancer: A phase I feasibility study. *Clin Cancer Res*. 2017;23:2730-2741.

15. Hartmans E, Tjalma JJJ, Linssen MD, et al. Potential red-flag identification of colorectal adenomas with wide-field fluorescence molecular endoscopy. *Theranostics*. 2018;8:1458-1467.

16. Ter Weele EJ, Terwisscha van Scheltinga AGT, Linssen MD, et al. Development, preclinical

safety, formulation, and stability of clinical grade bevacizumab-800CW, a new near infrared fluorescent imaging agent for first in human use. *Eur J Pharm Biopharm*. 2016;104:226-34.

17. Adsay NV, Basturk O, Saka B, et al. Whipple made simple for surgical pathologists: orientation, dissection, and sampling of pancreaticoduodenectomy specimens for a more practical and accurate evaluation of pancreatic, distal common bile duct, and ampullary tumors. *Am J Surg Pathol*. 2014;38:480-93.
18. Hoogstins CES, Boogerd LSF, Sibinga Mulder BG, et al. Image-guided surgery in patients with pancreatic cancer: first results of a clinical trial using SGM-101, a novel carcinoembryonic antigen-targeting, near-infrared fluorescent agent. *Ann Surg Oncol*. 2018;25:3350-3357.
19. Tummers WS, Miller SE, Teraphongphom NT, et al. Intraoperative pancreatic cancer detection using tumor-specific multimodality molecular imaging. *Ann Surg Oncol*. 2018;25:1880-1888.
20. Koller M, Hartmans E, de Groot DJA, et al. Data-driven prioritization and review of targets for molecular-based theranostic approaches in pancreatic cancer. *J Nucl Med*. 2017;58:1899-1903.
21. de Geus SWL, Boogerd LSF, Swijnenburg R-J, et al. Selecting tumor-specific molecular targets in pancreatic adenocarcinoma: paving the way for image-guided pancreatic surgery. *Mol Imaging Biol*. 2016;18:807-819.
22. Hiroshima Y, Maawy A, Zhang Y, et al. Metastatic recurrence in a pancreatic cancer patient derived orthotopic xenograft (PDOX) nude mouse model is inhibited by

neoadjuvant chemotherapy in combination with fluorescence-guided surgery with an anti-CA 19-9-conjugated fluorophore. *PLoS One*. 2014;9:1-13.

23. Hiroshima Y, Maawy A, Zhang Y, et al. Fluorescence-guided surgery in combination with UVC irradiation cures metastatic human pancreatic cancer in orthotopic mouse models. *PLoS One*. 2014;9:1-9.

24. Hiroshima Y, Maawy A, Zhang Y, et al. Fluorescence-guided surgery, but not bright-light surgery, prevents local recurrence in a pancreatic cancer patient derived orthotopic xenograft (PDOX) model resistant to neoadjuvant chemotherapy (NAC). *Pancreatology*. 2015;15:295-301.

25. Parsons CM, Sutcliffe JL, Bold RJ. Preoperative evaluation of pancreatic adenocarcinoma. *J Hepatobiliary Pancreat Surg*. 2008;15:429-35.

26. Handgraaf HJM, Boonstra MC, Prevoo HAJM, et al. Real-time near-infrared fluorescence imaging using cRGD-ZW800-1 for intraoperative visualization of multiple cancer types. *Oncotarget*. 2017;8:21054-21066.

27. Guolan L, van den Berg NS, Martin BA, et al. Tumour-specific fluorescence-guided surgery for pancreatic cancer using panitumumab-IRDye800CW: a phase 1 single-centre, open-label, single-arm, dose-escalation study. *Lancet Gastroenterol Hepatol.* 2020;5:753-764.

TABLES

Table 1. Patient and tumor characteristics

Patient					Tumor		
Dose	Nr.	*Age*	*Sex*	*WHO-score*	*Histology*	*TNM Stage*	*Radicality*
4.5mg	1	64	Female	0	Distal cholangiocarcinoma	pT3N1	R0
	2	67	Male	1	PDAC	pT3N1	R0
	3	75	Male	0	PDAC	pT3N0	R0
	4	69	Male	1	Auto immune pancreatitis	-	-
10mg	5	56	Male	1	Ampullary carcinoma	pT3N1	R0
	6	73	Female	0	PDAC	pT3N1	R1
	7	74	Female	0	Intrapapillar mucinous neoplasm	-	R0
25mg	8	47	Female	0	PDAC	pT3N2	R0
	9	74	Female	0	Ampullary carcinoma	pT3N1	R1
	10	67	Male	0	Neuroendocrine tumor	pT3N0	R0

Abbreviations: PDAC, pancreatic ductal adenocarcinoma; WHO, World Health Organisation; R0, radical resection; R1, not radical.

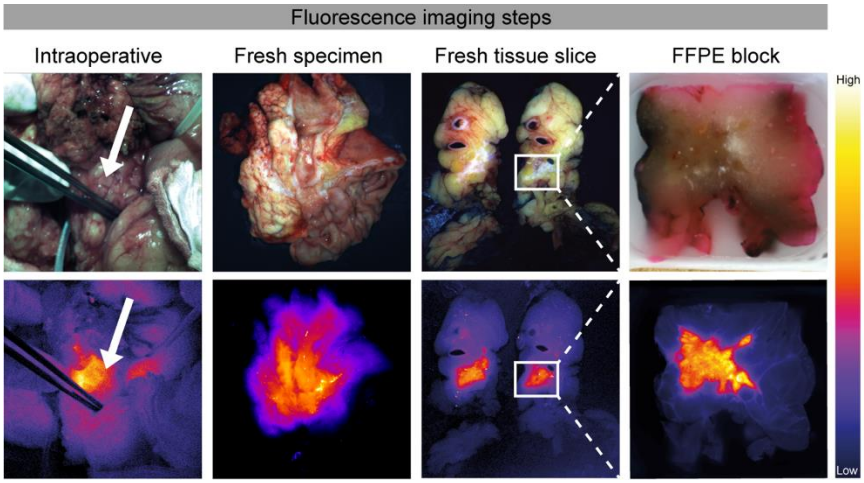

Figure 1: The workflow from intraoperative to FFPE blocks enabling correlation of intraoperative fluorescence signals with histopathology.

Intraoperative color images and corresponding fluorescence images are obtained in vivo during surgery. Then, imaging of the fresh surgical specimen, followed by serially slicing is performed. Imaging of the fresh tissue slices is followed by paraffin embedding. Imaging of formalin-fixed paraffin-embedded (FFPE) blocks is done to determine tumor-to-background ratio.

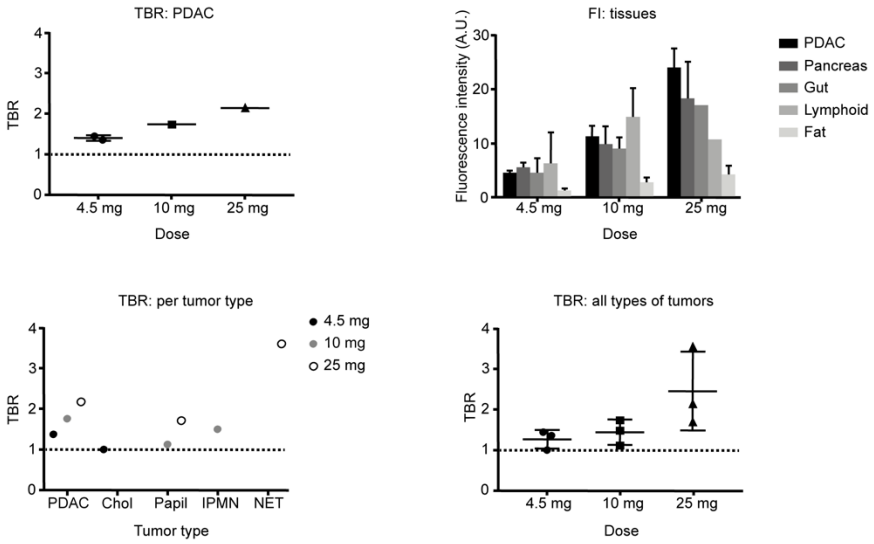

Figure 2. Tumor-to-background ratios (TBR) and fluorescence intensity (FI)

In the first row TBRs of all pancreatic ductal adenocarcinomas (PDAC) distributed per dose group and fluorescence intensity of different tissue types in patients with PDAC are shown. In the second row, mean TBR per tumor type distributed per dose group and mean TBRs of all types of tumors distributed per dose group are shown. Abbreviations: Chol, distal cholangiocarcinoma; IPMN, intraductal papillary mucinous neoplasm; NET, neuroendocrine tumor; Papil, ampullary carcinoma; PDAC, pancreatic ductal adenocarcinoma.

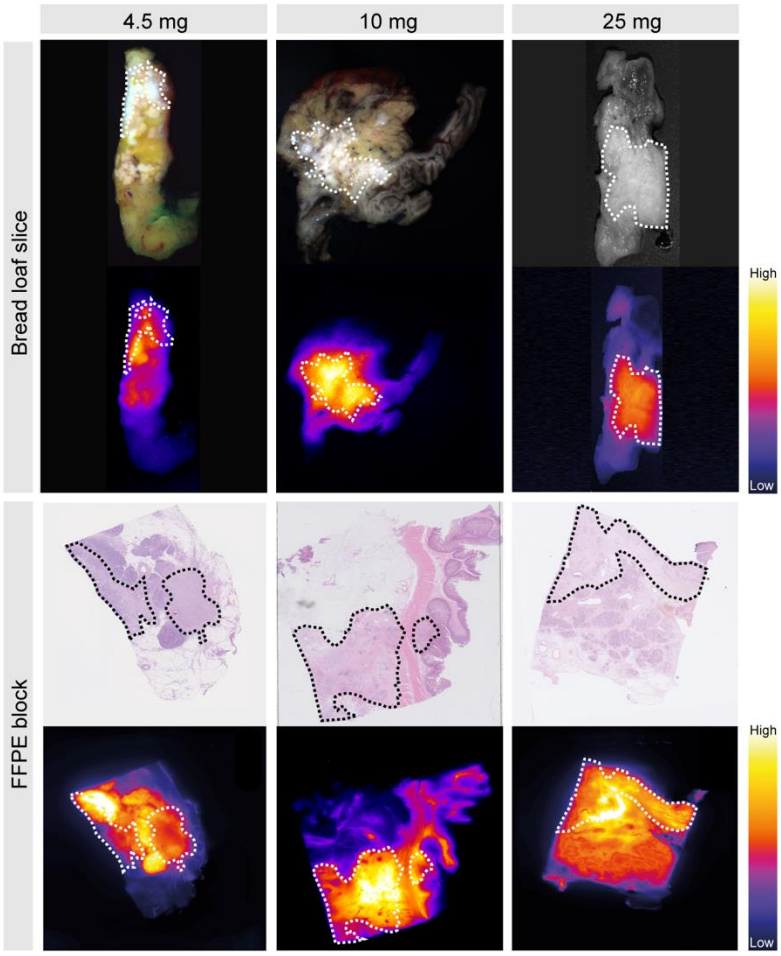

Figure 3: Representative images per dose group of pancreatic ductal adenocarcinoma.

Columns represent the three dose groups: 4.5 mg, 10 mg and 25 mg. Rows represent the imaging modality. In first row a white light image and below the corresponding representative fluorescence image. The third row contains the hematoxylin and eosin (H&E) sections and below the corresponding representative fluorescence image. Tumor tissue is delineated with a white or black dashed line. Abbreviations: FFPE, formalin-fixed paraffin-embedded.

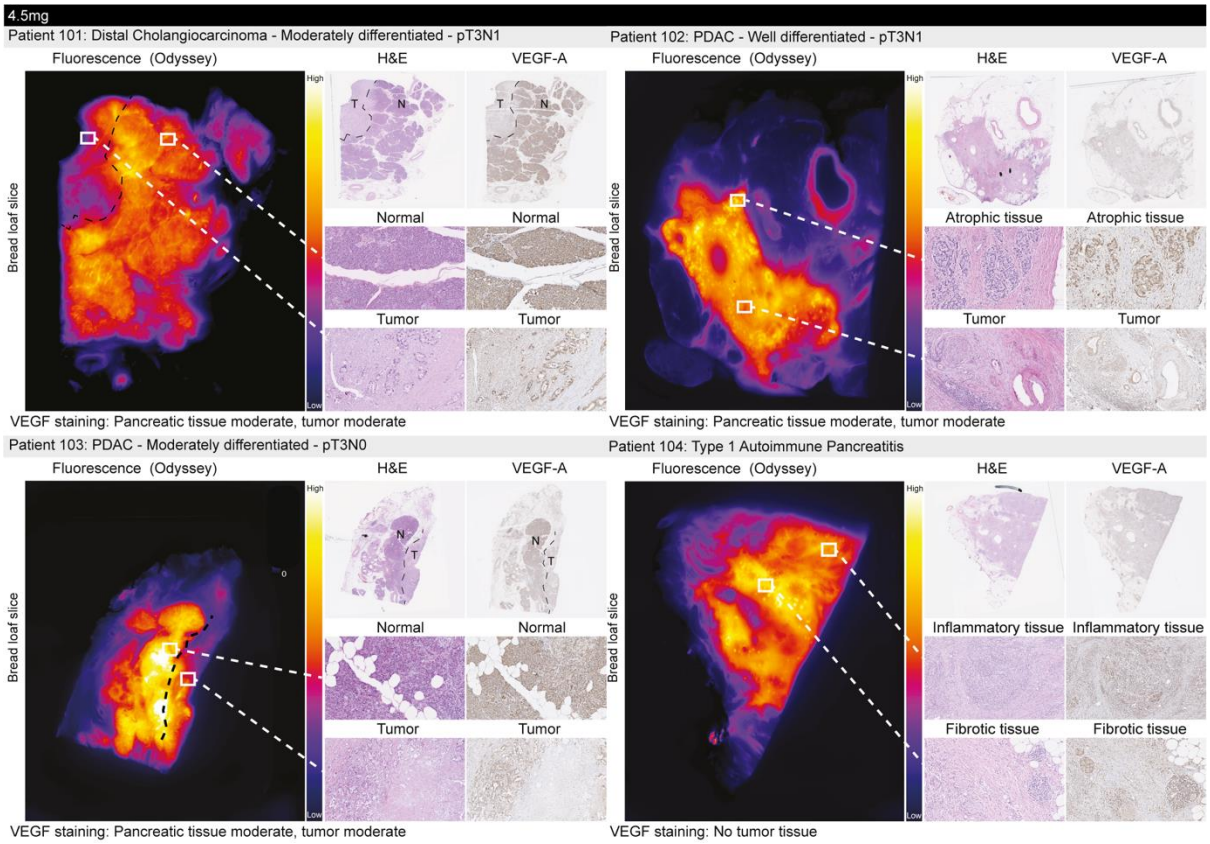

Figure 4: Representative fluorescence and histopathological images of each patient in the 4.5mg cohort.

The figure contains images of the patients included in the 4.5mg group. T is the area in images that contain tumor, N normal pancreatic tissue. Included per patient is a fluorescence image of the bread loaf slice, an image of the H&E staining of the bread loaf slice and an image of the VEGF-A staining of the bread loaf slice. Close-ups of the H&E staining and VEGF-A staining are also shown.

Tumor tissue is delineated, when possible, with a black dashed line. Abbreviations: PDAC, pancreatic ductal adenocarcinoma.

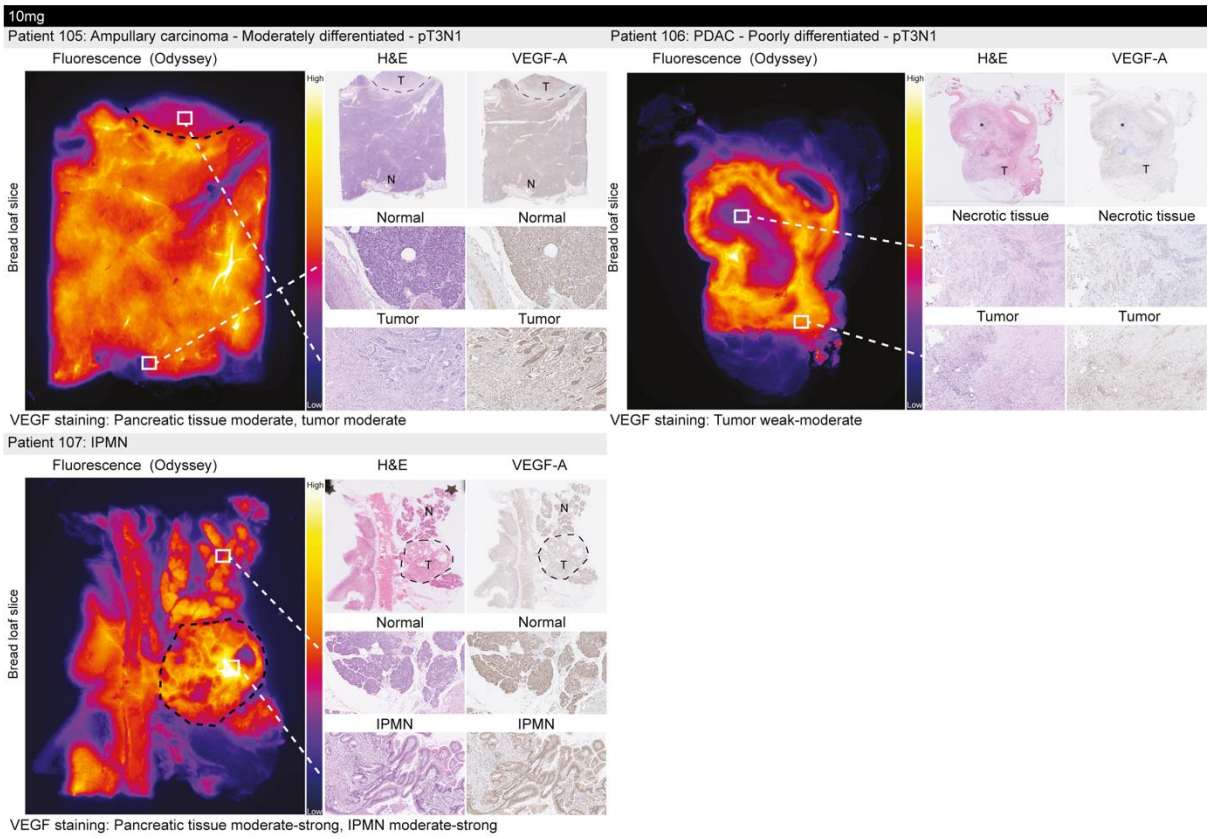

Figure 5: Representative fluorescence and histopathological images of each patient in the 10mg cohort.

The figure contains images of the patients included in the 10mg group. T is the area in images that contain tumor, N normal pancreatic tissue. Included per patient is a fluorescence image of the bread loaf slice, an image of the H&E staining of the bread loaf slice and an image of the VEGF-A staining of the bread loaf slice. Close-ups of the H&E staining and VEGF-A staining are also shown.

Tumor tissue is delineated, when possible, with a black dashed line. Abbreviations: IPMN, intraductal papillary mucinous neoplasm; PDAC, pancreatic ductal adenocarcinoma.

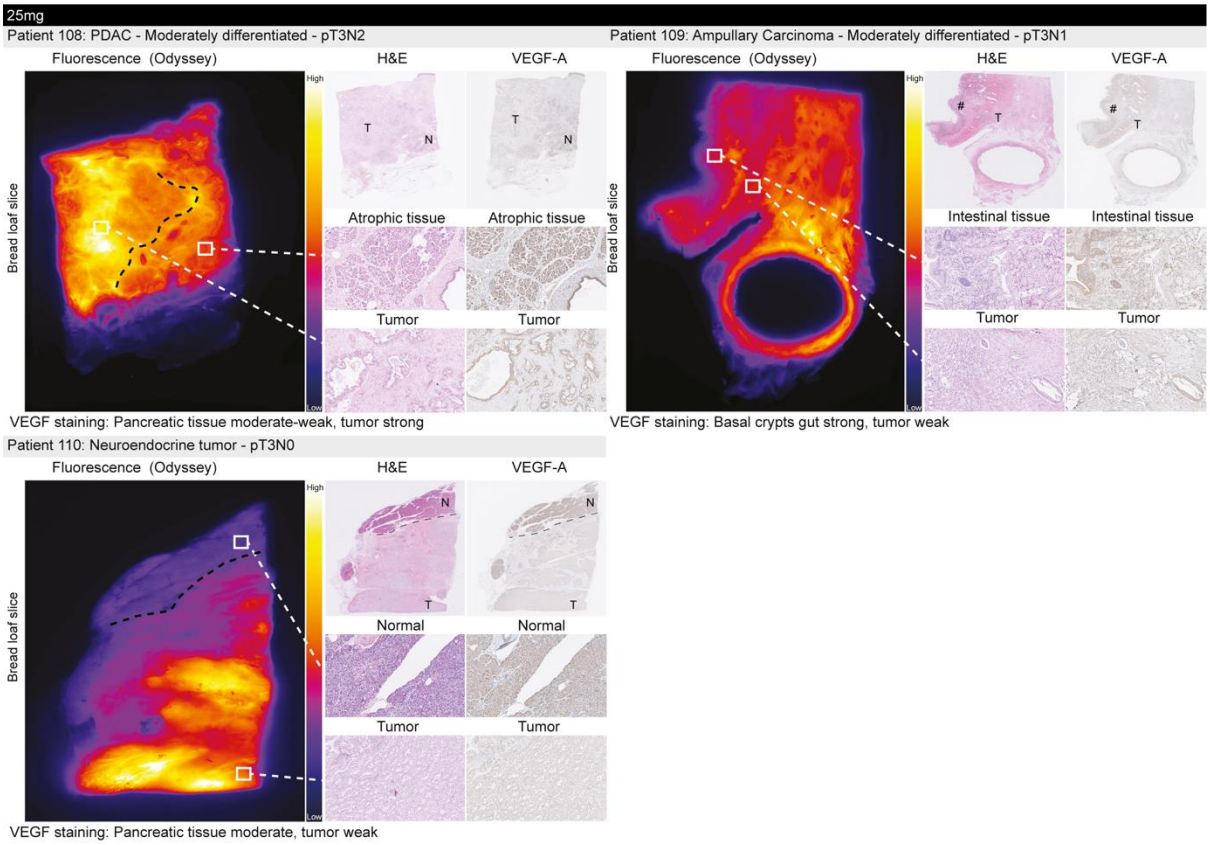

Figure 6: Representative fluorescence and histopathological images of each patient in the 25mg cohort.

The figure contains images of the patients included in the 25mg group. T is the area in images that contain tumor, N normal pancreatic tissue. Included per patient is a fluorescence image of the bread loaf slice, an image of the H&E staining of the bread loaf slice and an image of the VEGF-A staining of the bread loaf slice. Close-ups of the H&E staining and VEGF-A staining are also shown.

Tumor tissue is delineated, when possible, with a black dashed line. Abbreviations: PDAC, pancreatic ductal adenocarcinoma.

GRAPHICAL ABSTRACT

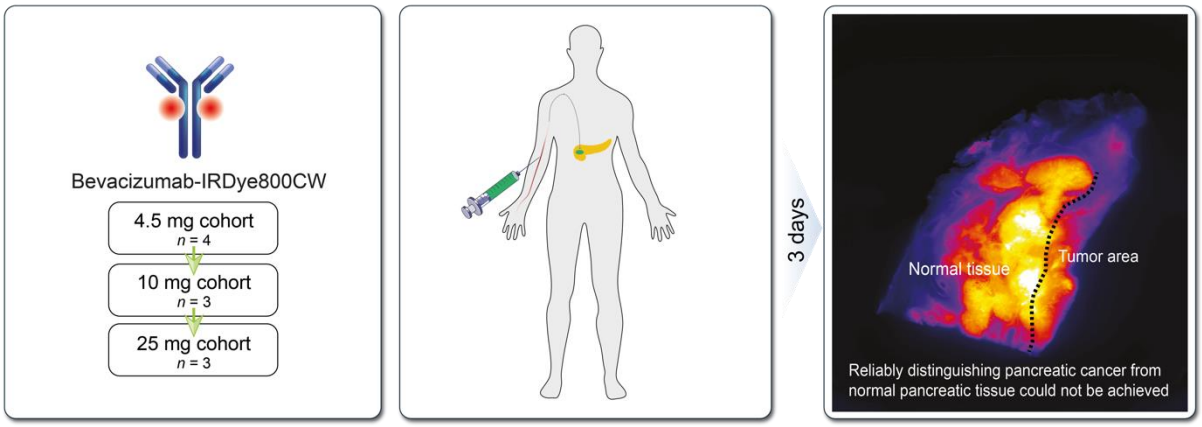

SUPPLEMENTAL INFORMATION

Investigational product

Bevacizumab-IRDye800CW was produced in the good manufacturing practice (GMP) facility of the UMCG by conjugating bevacizumab (Roche AG) and IRDye-800CW-NHS (LI-COR Biosciences Inc) under regulated condition. The average conjugation molecule ratio of bevacizumab to IRDye-800CW-NHS was 1:2, generating the conjugate bevacizumab-800CW. Vials containing 6.0mg bevacizumab 800CW dissolved in 0.9% sodium chloride (NaCl) solution were used to prepare the infusions in a concentration of 1mg ml^{-1}. After release of the final product by the certified qualified person at the UMCG GMP facility, the tracer was intravenously administered to the patients. The lower doses of 4.5 and 10mg were injected by slow bolus injection, and for 25 and 50mg an infusion pump was used (infusion speed: 150mL per hour). After injection the infusion line was flushed with 5 mL 0.9% NaCl.

Imaging system

Intraoperative imaging was performed using a fluorescence multispectral camera system dedicated to detect IRDye-800CW-NHS (SurgVision BV, Groningen, the Netherlands). The system was configured with two LED lights for 800 nm illumination and one LED light for white light illumination. Real-time color and NIR fluorescence images were acquired simultaneously. Fluorescence was detected using a highly sensitive electron-multiplying charge-coupled device (EMCCD) imaging sensor. In the color-NIR overlay images, 800 nm images were pseudo colored green. The working distance of the imaging system was 20 cm above the surgical field with a field of view of 15 cm × 15 cm, and a spatial resolution of ~2-line pairs per millimeter. For each experiment, settings were held constant on 50 ms exposure time and 300 gain; if fluorescence oversaturation occurred in higher dose groups we lowered the gain to 30 or 3 accordingly. Images were stored in raw Flexible Image Transport System (FITS) format. Before and after each surgical procedure the intraoperative camera system was calibrated using a calibration device

(CalibrationDisk, SurgVision BV, The Netherlands). The device consists of a disk with round windows that can hold 8 clear polypropylene tubes of 0.65 ml (Catalog #15160, Sorenson, BioScience, Inc, Murray, U.S.A.). The tubes were filled with 2% intralipid and two-fold increasing concentrations of bevacizumab-800CW from 1:6400 till 1:100 including one tube without tracer. The CalibrationDisk was used to test the system prior to and after surgery, whether low and high fluorescent signals could be detected from dilutional series and whether the system was functioning appropriately. A sterile transparent drape (Carl Zeiss Vision BV, Oberkochen Germany) covered the camera during surgery. The imaging device was approved for intraoperative application in humans by the technical departments of the UMCG and LUMC.

Fluorescence imaging systems for ex vivo imaging

After resection, fluorescence imaging of the resected specimen (before and after slicing) was performed in the pathology department. Imaging of the surgical specimen and slices was performed using the Blackbox (SurgVision BV, The Netherlands) or the Pearl imager (LI-COR, Lincoln, NE, USA). Both devices are light-tight macroscopic fluorescence imaging systems designed for ex vivo fluorescence imaging. We used the Odyssey® CLX fluorescence flatbed scanning system (LI-COR Biosciences Inc. Lincoln, Nebraska) for detecting fluorescence in formalin-fixed paraffin-embedded (FFPE) blocks.

Imaging procedures of the fresh surgical specimen

All the procedures took place in an environment as dark as possible, to prevent photobleaching of the tracer. The fresh surgical specimen is handled according to standard procedures. Upon arrival at the pathology department, the fresh surgical specimen was imaged in a light-tight macroscopic fluorescence imaging device. The whole specimen was inked according to protocols with black, red, green and blue ink. Subsequently, the fresh specimen was axially sliced according to Verbeke's protocol. Before formalin fixation, all slices were imaged on the ventral and dorsal sides in a light-tight macroscopic

fluorescence imaging system. Thereafter, the fresh tissue slices were fixed in formalin. After two days, the pathologist submitted tissue samples according to standard protocols. This study was performed without altering the standard operating procedures and therefore the pathologists were blinded to the fluorescent signal. Once the specimen was submitted, additional tissue samples were embedded whenever high fluorescence signals were detected in regions that would not have been yet embedded. The additional tissue block IDs were marked on a printed photograph of the tissue slices, to enable direct correlation between fluorescence signals in fresh tissue slice images and histology.

Imaging procedures of formalin-fixed tissue

All FFPE blocks of all patients were requested from the pathology department and were scanned with the Odyssey® CLX fluorescence flatbed scanning system using the same imaging settings (wavelength: 800 nm, resolution 21 µm, quality: medium, intensity. Afterwards, tissue slides were cut and stained with hematoxylin/eosin (H/E) to enable direct correlation between fluorescence signal and histology. H/E slides were digitalized using a digital slide scanner (Hamamatsu, Japan).

Macro-segmentation of the fresh tissue slices

We used images of the FFPE blocks of all patients to determine the TBR per patient. TBR was defined as the mean fluorescence intensity (MFI) measured in pancreatic cancer tissue divided by the MFI in surrounding tissue at macroscopic level. The distance from stage to camera was equal in all patients, and no ambient light influenced the fluorescent signals. All raw (FITS-format) fluorescence images of fresh tissue slices that contained tumor tissue were imported in ImageJ (Fiji, version 1.0). Regions Of Interest (ROI) were defined and correlated to the microscopic images. ROIs of the total tumor tissue area, as well as the total background tissue per fresh tissue slice are defined by the researcher involved (B.K.P.) and drawn manually. Mean fluorescence intensities (MFI, arbitrary units) of all fresh tumor tissue slices were measured per ROI and averaged per tissue type per patient, resulting in a MFI of

tumor tissue and MFI of background tissue per patient. The TBR was calculated for each patient by dividing the MFI of tumor tissue by the MFI of surrounding healthy tissue. After each dose group was finished, MFI of tumor tissue, MFI of healthy surrounding tissue and TBR for each patient were plotted in graphs (GraphPad Prism, version 7.0).

Immunohistochemical staining protocol for VEGF (paraffin slides)

The following steps were used for VEGF-A staining. First the slides were deparaffinised using xylene (2x5minutes) and air dried. Endogen peroxidase blocking was performed using (4·5 ml 30% H202 in 45·5 ml PBS) for 30 minutes followed by incubation with polyclonal rabbit anti-human VEGF-A (RB9031, ThermoScientific) (1:300). This was followed by poly-HRP-anti Ms/Rb/Rt IgG (BrightVision) staining (2x30 minutes) at room temperature and the peroxidase reaction using diaminobenzidine for 10 minutes. Between all the steps PBS was used for washing the slides except after the peroxidase reaction, when distilled water was used (3x5 minutes). A counterstaining was performed using Mayer's hematoxylin followed by dehydration with alcohol (70%-96%-100%). After air-drying (30 minutes), the slides were embedded using mounting media.

SUPPLEMENTAL TABLES

Cohort	(S)AE	CTCAE	Description	Moment	Related to tracer
Cohort I	AE	2	Bleeding drain entrance	Post-operative	Not likely
Cohort I	AE	3	Wound infection	Post-operative	Not likely
Cohort I	None				
Cohort I	AE	3	Cholangitis	Pre-operative	Not likely
Cohort I	None				
Cohort II	AE	2	Gastroparesis	Post-operative	Not likely
	AE	1	Wound healing disorder	Post-operative	Not likely
	SAE	4	Bleeding a. gastroduodenalis	Post-operative	Not likely
	SAE	3	Anastomotic leakage	Post-operative	Not likely
Cohort II	AE	1	Acute dyspnoea	Post-operative	Not likely
Cohort II	AE	2	SIRS-response	Post-operative	Not likely
Cohort III	None				
Cohort III	None				
Cohort III	None				

Supplemental Table 1. Safety data: Overview of (serious) adverse events ((S(AE) per dose group. Cohort I:4.5mg, Cohort 2: 10mg, Cohort III: 25mg. Abbreviations: CTCAE; common terminology for adverse events, grade 1: mild, grade 2: moderate, grade 3: severe, grade 4: life-threatening, grade 5: death. SIRS; systemic inflammatory response syndrome.

SUPPLEMENTAL FIGURES

Supplemental figure 1: Representative images of VEGF-A and HIF1-alpha immunohistochemistry staining

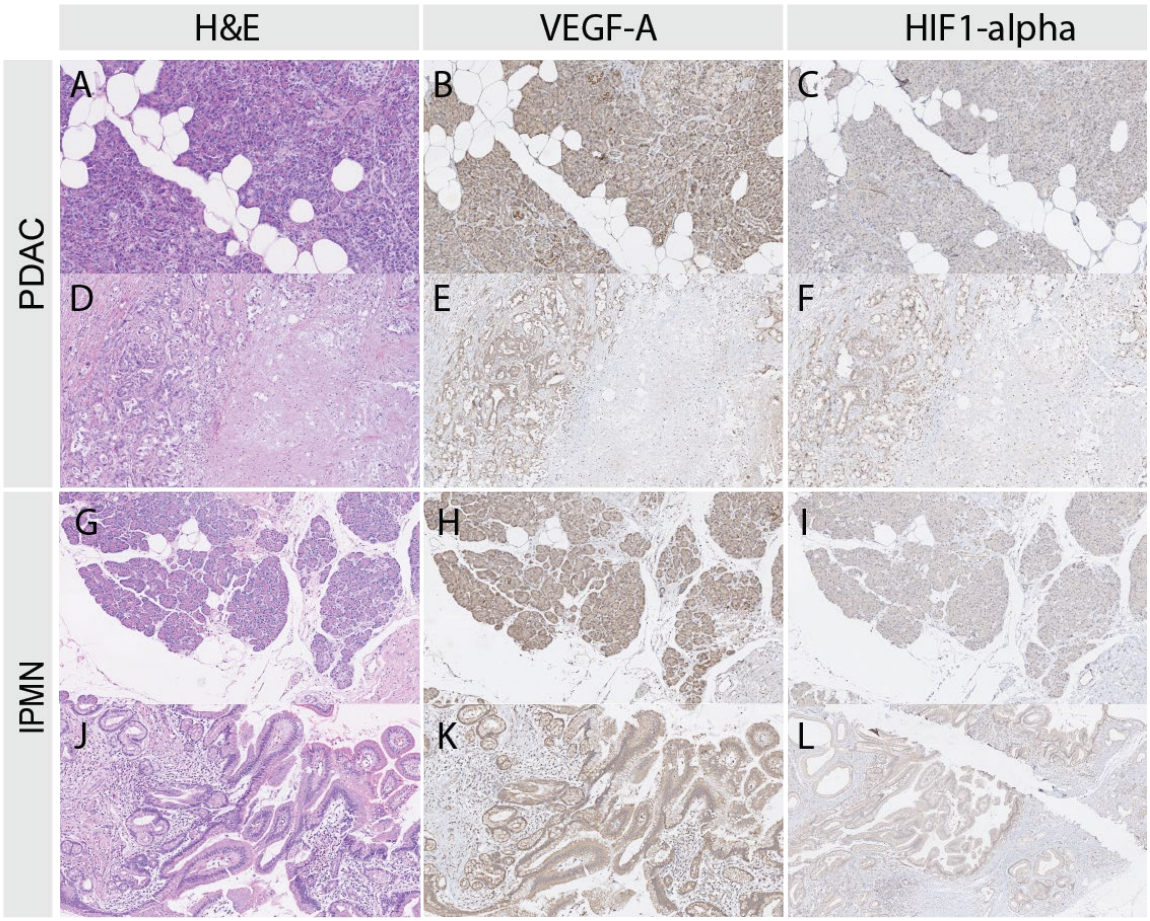

A-C: normal pancreatic tissue in a PDAC patient stained with H&E, VEGF, and HIF1-alpha. **D-F**: tumor tissue in a PDAC patient stained with H&E, VEGF, and HIF1-alpha. **G-I**: normal pancreatic tissue in a patient with IPMN stained with H&E, VEGF, and HIF1-alpha. **J-L**: tumor tissue in a patient with IPMN stained with H&E, VEGF, and HIF1-alpha. Abbreviations: H&E; hematoxylin and eosin, IPMN; intraductal papillary mucinous neoplasm, PDAC; pancreatic ductal adenocarcinoma, VEGF; vascular endothelial growth factor